# SPEED SENSORLESS CONTROL OF INDUCTION MOTORS BASED ON MCA EXIN PISARENKO METHOD

Binying Ye[*], STUDENT MEMBER IEEE
Maurizio Cirrincione[*/**], SENIOR MEMBER IEEE
(*) Université de Technologie de Belfort-Montbéliard
(UTBM)-OPERA, Belfort, France
binying.ye@utbm.fr
(**)University of the South Pacific (USP)
Suva,Fiji
m.cirrincione@ieee.org

Marcello Pucci#, SENIOR MEMBER IEEE,
Giansalvo Cirrincione[##], SENIOR MEMBER IEEE
(#) Institute of Intelligent Systems for the Automation,
Palermo (ISSIA-CNR), Italy
marcello.pucci@ieee.org
([##]) Université de Picardie Jules Verne
(UPJV), Amiens, France
g.cirrincione@ieee.org

***Abstract*—This paper proposes a speed sensorless technique for high performance induction motor drives based on the retrieval and tracking of the rotor slot harmonic. First, two cascaded ADALINEs (Adaptive Linear Elements) are used to extract the rotor slot harmonic (RSH) from the stator phase current signature, acting as adaptive filters, respectively in configuration band and notch, whose output consists of the RSH. Second, the MCA EXIN neurons are used to extract the eigenvector corresponding to the minimum eigenvalue of the autocorrelation matrix, which is formed by the ADALINEs' output sequence. Then, the slot frequency is estimated by using Pisarenko's theory with this retrieved minimum eigenvector, and subsequently the speed of the motor is estimated. Compared to the original Pisarenko's method however, not only the proposed algorithm can work recursively sample by sample, but the computational complexity and mean square frequency estimation error are largely reduced. The proposed sensorless technique has been experimentally tested on a suitably developed test set-up with a 2-kW induction motor drive. It has been verified that this algorithm can track the rotor speed rapidly and accurately in a very wide speed range, working from rated speed down to 1.3 % of it.**

***Keywords—induction motor; neural networks (NNs); minor component analysis (MCA); neural adaptive filtering; sensorless control***

## I. INTRODUCTION

Literature about sensorless control of induction motor (IM) drives is huge [1-21]. The sensorless techniques for IM can be mainly divided into two categories: methodologies based on fundamental models [3-7] and methodologies based on anisotropies models [8-13]. The former, such as model reference adaptive systems (MRAS) and observers in the synchronous or stationary reference frame, give good results in middle and high speed ranges, but they suffer problems at low speeds where the back EMF fades out, and the performance is highly affected by the variation of the machine parameters. Conversely, the latter, which track the machine saliencies, overcome these issues : they are generally implemented by the injection of a high frequency voltage or current carrier, needed to excite the saliency itself [8-12]. A different approach lies in trying to track the rotor slotting effect directly, without any high frequency carrier excitation [13-21].

The spectral components of rotor slot harmonics (RSHs) that can be observed in the stator phase current are given by [22],

$$f_h = \left(r\, q_r \mp n_d / n_p\right)\left(1-s\right) f_1 \mp \nu\, f_1 \tag{1}$$

With $f_1$ is the fundamental harmonic of the supply voltage, $s$ the slip, $p$ the number of pole pairs; $n_d$ the eccentricity order, $r$ the order of the space harmonic; $\nu$ is the order of the stator time harmonics present in the power supply driving the motor, $q_r$ the number of rotor slots per pole pair. It should be noted, however, that the harmonics described in (1) are not present in a real machine for any combination of the number of rotor slots and pole pairs [21-22]; finally, the upper sign refers to the case $q_r=3n-1$, and the lower one to the case $q_r = 3n + 1$, with $n \in$ N. In this analysis the stator slots for phase are supposed $3n$, so no stator slot harmonics are present and the information in the stator current is due only to the rotor slot harmonics.

The principal slot harmonic (PSH) refers to the first and prominent harmonic in the PSH series for an IM, obtained from eq. (1). With $\nu$=1, $r$=1, and $n_d$=0, and if the time harmonics of the stator and rotor currents, the static and if dynamical eccentricities are neglected, then the PSH is given by

$$f_h = q_r f_1 \left(1-s\right) \mp f_1 \tag{2}$$

As compared to the fundamental frequency, it can be found from (2) that the PSH appears at rather high ranges of the current spectrum at no-load; however, under load conditions, rotor slot harmonics move away from the one at no-load, reducing (increasing) the value of the frequency for positive (negative) loads. This implies that the PSH tends to

confuse with other harmonic already present in the IM ($5^{th}$, $7^{th}$ etc), especially at low speed; consequently the PSH is harder to be identified.

It is apparent that the frequencies given by (1) (2) depend on the machine load, because of the slip. In other words, the position of PSH in the stator-current spectrum is tied to the rotor speed tightly, that's why slot harmonics have found wide application in speed detection in sensorless drives.

These harmonics can be exploited to successfully retrieve the instantaneous value of the rotor speed and position, since the other parameters in (1) and (2) are either known or constant. This avoids increasing acoustic noise and losses caused by injected signals, and simplifies the signal processing system. As far as the direct PSH tracking is concerned, two main approaches have been generally followed in literature:

- Frequency domain methods, mainly based on FFT (Fast Fourier Transform)-like approaches [15-18];
- Time domain methods, most of which are PLL (Phase-Locked Loop)-like approaches [19-21].

In general, most frequency domain methods are modified versions of the traditional discrete Fourier transform (DFT) or other spectrum-estimation techniques: as is known, they have a good accuracy and linearity over a very wide speed range and load conditions, but a compromise has to be made between the required frequency resolution and the response time. While the time domain methods, such as PLL, generally provide a better real-time performance, however the accuracy of the result is more susceptible to the noise. However, to track the time varying PSH, both accuracy and speed of response are required.

This paper, proposes a speed estimation method based on ADALINE (ADAptive LINear Element) [23-25] and minor component analysis (MCA), particularly by using the MCA EXIN neurons [26], which allows obtaining a higher resolution with the same sampling frequency in a very wide frequency range. The overall system combines the advantages of both the frequency domain methods (accuracy) and the time domain methods (speed of response). Besides that, the MCA explores the orthogonality between the noise subspace and the signal subspace, its effectiveness is guaranteed even when the signal-to noise ratio is low.

The proposed method can continuously and accurately track the rotational speed of IM at both dynamic or steady-state conditions, and the centre frequency does not have to be changed manually at each computation cycle. It has been implemented on a rotor flux oriented controlled drive and experimentally tested on a suitably developed test set-up with a 2-kW induction motor.

This paper is organized as follows. The cascaded ADALINEs structure which is used to extract the rotor slot harmonic from the stator phase current, is described in section II. The Pisarenko's theory and the corresponding MCA EXIN neural solution are introduced in Section III and IV. Finally, experimental results to confirm the viability of the method are provided in Section VI.

## II. RETRIEVE OF ROTOR SLOT HARMONICS

### A. Adaptive Linear Neural Filter

An adaptive linear neural filter based on a linear adaptive neuron (ADALINE) with two adaptive weights has been adopted to retrieve the rotor slot harmonics from the stator current signature, as shown in fig. 1. It is used as a notch filter or a band filter [23-25]. This means that the neuron is either able to cancel a determined signal at a certain frequency (notch filter), or it is able to let a determined signal pass at a predefined frequency (band filter, where band stands for a band of signals in a very narrow range around a predefined frequency).

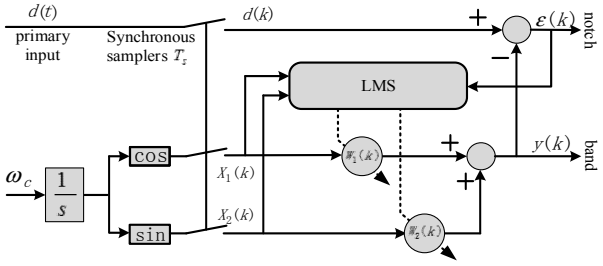


Fig. 1. Schematic representation of the ADALINE

The ADALINE network presents two inputs and two outputs: the primary input is the signal to be processed, which is assumed to be of any kind of signal; the reference input is a pure cosine wave and its $\pi/2$ delay, at the frequency $\omega_c$ of the primary input signal $d(k)$ that should be eliminated or let pass; the two outputs give the notch and the band behaviour respectively.

The sampled reference inputs are therefore,

$$\begin{cases} x_1(k) = C\cos(k\omega_c + \varphi) \\ x_2(k) = C\sin(k\omega_c + \varphi) \end{cases} \tag{3}$$

where C is the amplitude of the sinusoidal sequence with reference frequency $\omega_c$, and $k$ is the current sampled time.

The procedure for updating the weights is a least-squares algorithm (LS), such as the LMS or the TLS algorithm [26][27]. The LMS is adopted here because of its low complexity, low computational demand, and high-speed of convergence. Its learning laws are shown beneath:

$$\begin{cases} w_1(k+1) = w_1(k) + 2\mu\varepsilon(k)x_1(k) \\ w_2(k+1) = w_2(k) + 2\mu\varepsilon(k)x_2(k) \end{cases} \tag{4}$$

Where

$w_i(k)$ the weight of the $i^{th}$ neuron at the $k^{th}$ time sample;

$\mu$ the learning rate;

$\varepsilon$(k) the difference between the primary input signal $d(k)$ and the band filter output $y(k)$; □(k) is also the notch filter output.

The corresponding band transfer function $K(z) = y(z)/d(z)$ and notch transfer function $H(z) = \varepsilon(z)/d(z)$ are given respectively as,

$$K(z) = \frac{2\mu C^2 (z\cos(\omega_c) - 1)}{z^2 - 2(1-\mu C^2) z\cos(\omega_c) + 1 - 2\mu C^2} \quad (5a)$$

$$H(z) = \frac{z^2 - 2z\cos(\omega_c) + 1}{z^2 - 2(1-\mu C^2) z\cos(\omega_c) + 1 - 2\mu C^2} \quad (5b)$$

where $\varepsilon(z)$and $d(z)$ are the $z$-transform of sequences $\varepsilon_k$ and $d_k$; the transfer functions represent typical second order adaptive filters, like the SOGI-FLL in [28-29]. The notch output and the band output are one complementary to the other.

Moreover it can be further derived by a simple analysis on the poles and zeros of the function, that the quality factor of the filter is explicitly related to the parameters as follows [24]

$$Q = \frac{\text{center frequency}}{\text{bandwidth}} = \frac{\omega_c}{2\mu C^2} \quad (6)$$

The bandwidth and centre frequency of the filter can be adjusted separately by the learning rate $\mu$ and $\omega_c$, and they completely define the dynamic and the filtering characteristics of the ADALINE filter.

*B. The Retrieval of the PSH by ADALINEs*

To retrieve the harmonic current $i_h$ due to the PSH from the stator phase current, the structure in Fig. 2 is proposed:

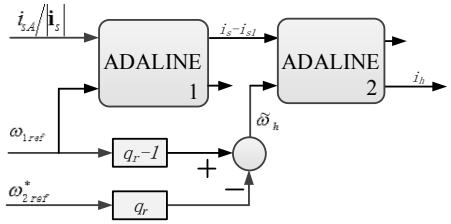


Fig. 2. Cascaded ADALINEs structure to track the PSH

Fig. 2 shows the overall PSH retrieval system based on two cascaded ADALINEs: one (ADALINE1) works in notch mode to eliminate the fundamental harmonic, the other (ADALINE2) works in band mode to retrieve the PSH. This structure is particularly effective at very low speed range, as the PSH become closer to the fundamental harmonic: in this case indeed a mere filtering approach in band mode can be hardly adopted, unless a very slow dynamic is accepted. A better way is to remove the fundamental component first as shown in fig. 2.

ADALINE1 receives as input the normalized stator phase current $i_{sA}(k)/|\mathbf{i}_s|$ given by

$$i_{sA}(k)/|\mathbf{i}_s| = \left[\sum_{\substack{n=1 \\ n\neq h}}^{\infty} I_n \cos(\omega_n k + \varphi_n)\right] + I_h \cos(\omega_h k + \varphi_h) \quad (7)$$

where $\omega_{1ref}$, is the supply fundamental angular frequency, $I_h$, $\omega_h$, $\varphi_h$ are respectively the amplitude, angular frequency and initial phase of the principal PSH, and $I_n$, $\omega_n$, $\varphi_n$ are respectively, the amplitude, angular frequency and initial phase of the harmonics not including the principal PSH.

The output of ADALINE1 is the current $i_s$-$i_{s1}$, that is the normalized stator phase current without the fundamental frequency.

The second ADALINE (ADALINE2) has this last signal as input as well as the $\omega_h$ frequency, i.e. the estimated slot frequency $\omega_h$, which is computed by using $\omega_{1ref}$ and the slip angular frequency $\omega_{2ref}$ as follows by using (2), thus under consideration is the principal rotor slot harmonic.

$$\tilde{\omega}_h = (q_r - 1)\omega_{1ref} - q_r\omega_{2ref} \quad (8)$$

ADALINE2 works in band mode and extracts the slot current $i_h$

$$i_h(k) = I_h \cos(\omega_h k + \varphi_h) \quad (9)$$

$\omega_{1ref}$ is generally the supply fundamental frequency of the inverter, and its value is given in the framework of the controllers: it is estimated by the so called "current" model of the induction motor on the basis of the vector product between the rotor flux space vector and its derivative [2].

The structure shown in fig. 2 works properly if the PSH is the largest signal once the fundamental frequency has been cancelled. However, $\omega_h$ must be provided quickly and this paper proposes to estimate the slip angular frequency on the basis of the so-called "current" model of the induction motor written in the rotor flux oriented reference frame (to avoid open-loop integration problems and reduce any sensitivity versus the stator resistance variation at low speed) [2]

$$\omega_{2ref} = \frac{L_m}{T_r|\boldsymbol{\Psi}_r|^2}(\psi_{rd} i_{sQ} - \psi_{rq} i_{sD}) = \frac{2R_r}{3|\boldsymbol{\Psi}_r|^2} t_e \quad (10)$$

where $i_{sD}$, $i_{sQ}$ are the stator currents components in the stator reference frame, $|\boldsymbol{\psi}_r|$ is the amplitude of the rotor flux and $\psi_{rd}$, $\psi_{rq}$ its components in the stator reference frame, $t_e$ is the electromagnetic torque, $L_m$ and $T_r$ are respectively the three-phase magnetizing inductance and the rotor time constant.

*C. Design Criteria*

The learning rate $\mu$ has to be set to obtain a good trade-off between the bandwidth and the convergence speed; this is crucial for the network performance and the overall stability of the system. As a matter of fact, a slow convergence, corresponding to a lower value of $\mu$ and a resulting narrower band, introduces a delay that, in a feedback action, could be unacceptable. In addition, filter stability considerations impose the upper limit of $\mu$ on the basis of the maximum eigenvalue of the autocorrelation matrix $\lambda_{max}$: $1/\lambda_{max} > \mu > 0$.

In particular, for the ADALINE in notch mode, the fundamental harmonic is expected be eliminated. It is assumed that the supply pulsation reference $\omega_{1ref}$ is close enough to the true fundamental frequency. Normally a greater $\mu$ is preferred, due to the resulting faster convergence and perfect elimination of the fundamental harmonic. This is not true however for low speed values and with heavy load: in these conditions, the principal PSH frequency is very close to the fundamental, and therefore a smaller $\mu$ can guarantee that the PSH is unaffected when the fundamental is cancelled. Fig.3 shows the frequency response of the ADALINE notch with respect to $\mu$.

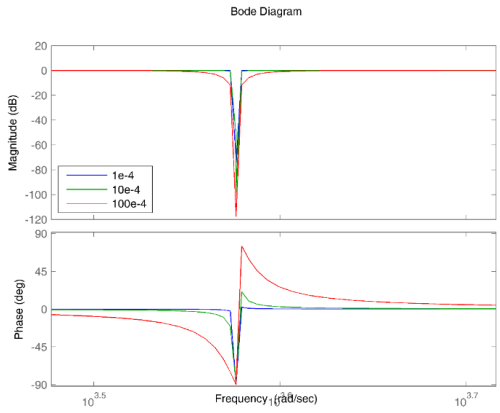


Fig. 3. frequency response of the ADALINE notch with respect to $\mu$, centered at 2π*600rad/s.($f_1$=50Hz, $s$=7.14% the experimental motor)

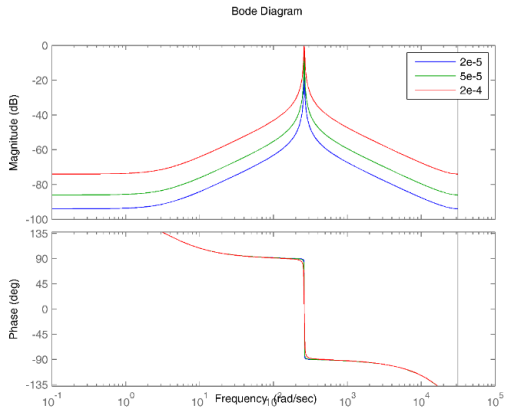


Fig. 4. frequency response of the ADALINE band with respect to $\mu$, centered at 2π*600rad/s.($f_1$=50Hz, s=7.14% the experimental motor)

For the ADALINE in band mode, the centre frequency is tuned according to the estimated $\omega_h$, therefore the bandwidth has to be wide enough to compensate the error between $\omega_h$ and the true one, permitting the system to track the PSH properly even in the presence of variations of the value given by (8). Moreover it has better phase characteristics around the band frequency than the notch filter. On the other hand, it is important that the harmonic and inter-harmonics around the PSH be lying outside the bandwidth of the filter, and this requires a low value of $\mu$. Since in real drive systems, the PSH varies quickly according to the working conditions, and since the motor current signature is full of different time-variable harmonics, the constraints for the ADALINE in band mode are of utmost importance. Fig 4 shows the frequency response of the ADALINE in band mode with respect to $\mu$.

## III. The Pisarenko's theory

The noisy discrete-time measurements of the filtered slot harmonic from the ADALINEs can be represented as

$$x(k) = i_h(k) + q(k) = I_h \cos\left(\omega_h k + \varphi_h\right) + q(k) \qquad (11)$$

where $\omega_h$ is the slot harmonics pulsation, $\varphi$ is a random variable uniformly distributed in [-π,π]. The noise $q$(k) is assumed to be a zero-mean white process with unknown variance $\sigma^2$. The task is to find $\omega_h$ from $K$ samples of $x(k)$.

Many existing subspace methods, such as Pisarenko and MUSIC assume that the signal is a sum of harmonics and explore the orthogonality between the noise subspace and the signal subspace [30-32]. The frequency can be then computed simply by finding the eigenvectors corresponding to the smallest eigenvalues [30].

Among them, Pisarenko4s method is probably the most simple and computational efficient. In the Pisarenko's method [30], it is assumed that the data sequence is a sum of $p$ complex exponentials in white noise,

$$x(k) = \sum_{i=1}^{p} \mathbf{A}_i e^{j\omega_i k} + v(n) \qquad (12)$$

Where $v(n)$ is a zero mean white noise with variance $\sigma^2$, and $\mathbf{A}_i$, $\omega_i$ are respectively the amplitude and the angular pulsations of the $i^{th}$ exponential. The amplitudes $\mathbf{A}_i$ are complex numbers as follows:

$$\mathbf{A}_i = |A_i| e^{j\varphi_i} \qquad (13)$$

and the phases $\varphi_i$ are considered uncorrelated random variables uniformly distributed over the interval [-π, π).

In the Pisarenko's theory, the data sequence is considered to be a final length sequence of $M$=$p$+1 elements, therefore a ($p$+1)×($p$+1) autocorrelation matrix is constructed as follows:

$$\mathbf{R}_{xx} = E(\mathbf{x}\mathbf{x}^T) = \begin{bmatrix} r_{xx}(0) & r_{xx}(1) & \cdots & r_{xx}(p) \\ r_{xx}(1) & r_{xx}(0) & \cdots & r_{xx}(p-1) \\ \vdots & \vdots & \ddots & \vdots \\ r_{xx}(p) & r_{xx}(p-1) & \cdots & r_{xx}(0) \end{bmatrix} \qquad (14)$$

where $r_{xx}(k)$ is the $k^{th}$ input autocorrelation sequence such that

$$r_{xx}(k) = \mathrm{E}\{x(n+k)x^*(n)\} = \mathrm{E}\{x^*(n)x(n+k)\} = r_{xx}^*(-k) \qquad (15)$$

Where E is the expected value of x(k) random variable (ensemble average)

It is easy to prove that $\mathbf{R}_{xx}$ can be decomposed into

$$\mathbf{R}_{xx} = \mathbf{R}_{ss} + \sigma^2 \mathbf{I} \tag{16}$$

where $\mathbf{R}_{ss}$ is the autocorrelation matrix without noise.

The autocorrelation matrix $\mathbf{R}_{ss}$ is of rank $p$[30], but $\mathbf{R}_{xx}$ is of rank $p+1$ due to the presence of white noise, with eigenvalues $\sigma^2 \leq \lambda_p \leq \ldots \leq \lambda_1$ and corresponding orthonormal eigenvectors $\mathbf{z}_{p+1}$ , $\mathbf{z}_p, \ldots,$ $\mathbf{z}_1$. In Pisarenko's method, the dimension of noise subspace is equal to one, and it is spanned by the eigenvector corresponding to the minimum eigenvalue, $\lambda_{min} = \sigma^2$. Denoting this noise eigenvector by $\mathbf{v}_{min}$, it follows from (16) by multiplying $\mathbf{v}_{min}$ that

$$\mathbf{R}_{ss}\mathbf{v}_{\min} = 0 \tag{17}$$

And $\mathbf{v}_{min}$ is therefore orthogonal to each of the signal vectors, $e_i = \begin{bmatrix} 1 & e^{j\omega_i} & e^{j2\omega_i} & \cdots & e^{jp\omega_i} \end{bmatrix}^T$ [30]. Thus, the frequency can be estimated by finding all the roots of the following polynomial equation formed by the minimum eigenvector ($z$-transform),

$$V_{\min}(z) = \sum_{k=0}^{p} \mathbf{v}_{\min}(k) z^{-k} = \prod_{k=0}^{p} (1 - e^{j\omega_k} z^{-1}) \tag{18}$$

corresponding to the $p$ harmonics of the signal: the frequency amplitudes of the complex exponentials are therefore determined by the roots of $V_{min}(z)$. Also the signal frequencies can be extracted by taking the angles of the roots.

As the real-valued input $\cos(\omega t)$ is convenient to be represented as $(e^{j\omega t}+e^{-j\omega t})/2$, thus for a real-valued input which consists of $p$ harmonics, a $(2p+1)\times(2p+1)$ input autocorrelation matrix has to be constructed.

## IV. The MCA EXIN Pisarenko's method

The original Pisarenko method is limited by the estimation of the autocorrelation matrix and the eigen-decomposition (with $O(M^3)$ computational complexity) of this matrix. This will on the one hand bias the estimation results, and on the other hand prevents it from being used in real time applications. Nevertheless, the recursive MCA EXIN neuron, which deals with the recovery of the eigenvector corresponding to the minimal eigenvalue of the data sequence's autocorrelation matrix, as proposed in [26], can be adopted for finding the minimum eigenvalue and corresponding eigenvector to be used in Pisarenko's method. [27].

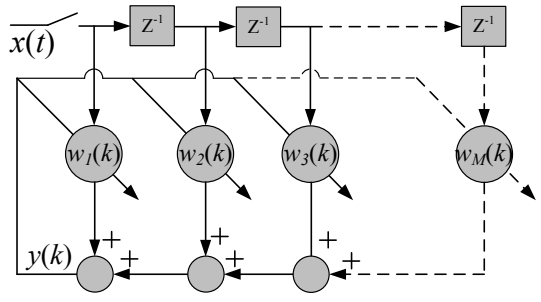


Fig. 5. The recursive linear MCA neural network

Let a linear neuron (see fig.5) be considered with a real number input vector $\mathbf{x}(k) = [x_1(k),\ldots, x_M(k)]^T$ and with output $y(k)$:

$$y(k) = \mathbf{w}^T(k)\mathbf{x}(k) = \sum_{i=1}^{M} w_i(k) x_i(k) \tag{19}$$

where $\mathbf{w}(k) = [w_1(k),\ldots, w_M(k)]^T$ is the weights vector.

In the application at hand the input vector $\mathbf{x}(k)$ is the output of ADALINE2 of fig.2, and in convergence the weights represent the components of the eigenvector corresponding to the minimum eigenvalue of the autocorrelation matrix of the input data. The output is the residual and in convergence goes to zero. Finally the dimension of the neural networks is chosen in accordance with the dimension of the autocorrelation matrix as detailed before.

**In order that the neural weights converge to the minimum eigenvector, the updates of the weights follow the gradient descent of the Rayleigh quotient (RQ) :**

$$E[J] = r[\mathbf{w}, \mathbf{R}_{xx}] = \frac{\mathbf{w}^T \mathbf{R}_{xx} \mathbf{w}}{\mathbf{w}^T \mathbf{w}} \tag{20}$$

The MCA EXIN, one of the best learning law in terms of stability and converging time, whose averaging gradient flow (ODE) is directly derived from discretization of the sequential version of the gradient flow of RQ [26],

$$\mathbf{w}(k+1) = \mathbf{w}(k) - \frac{\alpha(k) y(k)}{\|\mathbf{w}(t)\|^2} \left[ \mathbf{x}(k) - \frac{y(k)\mathbf{w}(k)}{\mathbf{w}^T(k)\mathbf{w}(k)} \right] \tag{21}$$

**where $\alpha(k)$ is the learning rate.**

Let $\mathbf{R}_{xx}$ be the $M\times M$ autocorrelation matrix of input data, then if $\mathbf{w}(0)$ satisfies $\mathbf{w}^T(0)\mathbf{z}_M \neq 0$ (being $\mathbf{z}_M$ the orthonormal eigenvector corresponds to the smallest eigenvalue), it holds that $\mathbf{w}(k)$ converges to $\pm\|\mathbf{w}(0)\|\mathbf{z}_M$, then this weight vector, which converges to the eigenvector corresponding to the smallest eigenvalue, can be used in (18) (to replace $\mathbf{v}_{min}$) for computing the frequencies of the p-complex frequencies present in the signal at the output of ADALINE2. It considered that as output of ADALINE2 only the complex exponential corresponding to the PSH is present (p=1) and therefore $M=2p+1=3$ samples are required and consequently only three weights, Once the MCA EXIN processes the signal, the weights give the eigenvector to be used by Pisarenko's method to retrieve the PSH.

## V. Test set-up

The proposed speed estimator has been verified in the experiment, the employed test set-up consists of:

- A three-phase induction machine with parameters shown in Tab.1, with 36 stator and 28 rotor slots.
- An 8 kVA, three-phase VSI for the control of the machine side inverter.
- A torque controlled brushless Interior Mounted Permanent Magnet (IMPM) machine drive for the load.

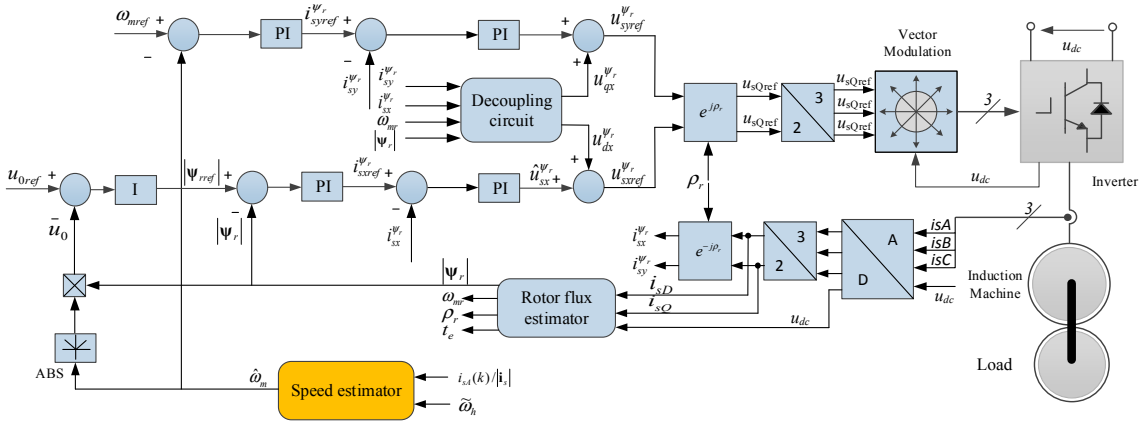


Fig. 6. Implement field oriented scheme and speed estimation scheme

- A dSPACE card (DS1103) with a PowerPC 604e at 400 MHz and a floating-point DSP TMS320F240 for the control of the machine side inverter.

TABLE I. PARAMETERS OF THE INDUCTION MACHINE

| | |
|---|---|
| Rated power Prated [kW] | 2.2 |
| Rated voltage Urated [V] | 220 |
| Rated frequency frated [Hz] | 50 |
| Pole-pairs | 2 |
| Stator resistance Rs [Ω] | 2.9 |
| Stator inductance Ls [mH] | 223 |
| Rotor resistance Rr [Ω] | 1.52 |
| Rotor inductance Lr [mH] | 229 |
| 3-phase magnetizing inductance Lm [mH] | 217 |
| Moment of inertia J [kg·m2] | 0.0048 |

## VI. RESULTS

The speed estimation performance is verified in the framework of the measured speed based vector control system: a VSI direct rotor-flux oriented vector control [field oriented control (FOC)] (as shown in fig. 6) in which current control is performed at the field reference frame level [2][22], the proposed speed estimator is connected on-line along with the main vector control loop, the variables $\omega_{1ref}$ and $\omega_{2ref}$, which are used for the reference of ADALINEs, are respectively taken from the PWM supply frequency and estimated by the "current" flux model based on the rotor equations of the machine written in the rotor flux oriented reference frame. The output of the estimator is fed back to close the speed control loop.

To verify the proposed speed estimation algorithm, the measured speed (from the encoder) is shown as comparison, along with the estimated speed. The test is made for different loads and speed conditions. The PSH frequency varies from hundreds of hertz to only a few hertz when the speed reference changes from rated speed (150 rad/s) to low speed (2 rad/s). The sampling frequency for the MCA EXIN Pisarenko's method is kept at 2.5k Hz. The following part only shows the results of the most challenging tests at low speeds.

Fig. 7 to fig.8.show the tracking capability results when the speed reference is a step from 5 rad/s (3.3% of the rated speed) to 10 rad/s (6.6% of the rated speed) with a 5Nm-load . This is a particularly challenging test since it implies a step variation at very low speed at almost the rated load torque.

Fig.7 a shows the corresponding estimated speed and the measured speed, respectively. Both the steady-state and transient performance are satisfactory, and in any case sufficient to close properly the speed loop of the drive. Remark that the estimated speed tracks the measured speed within 0.01s, which is hardly the case of these kind of algorithms Fig. 7 b shows the estimated PSH frequency from which the speed is computed.

Fig.8 presents the normalized phase current of the motor in the test. It can be observed from fig.8 a that the stator phase current is full of harmonics, while the waveform at the output of ADALINEs contains only the slot harmonics, as expected.

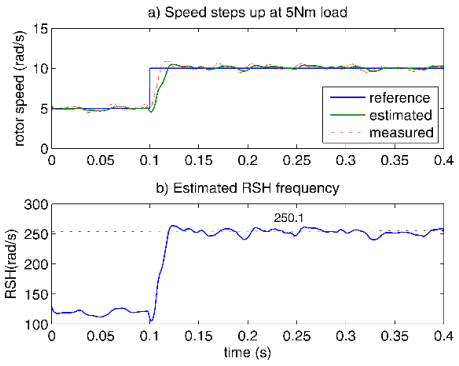


Fig. 7. Tracking capacity when speed step up at 5Nm load condition

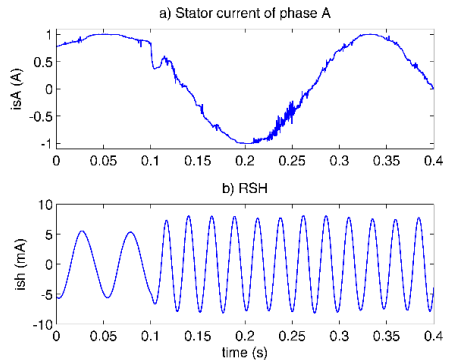


Fig. 8. Normalized phase current $i_{sA}$ and the output of filter $i_h$ when speed step up at 5Nm-load condition

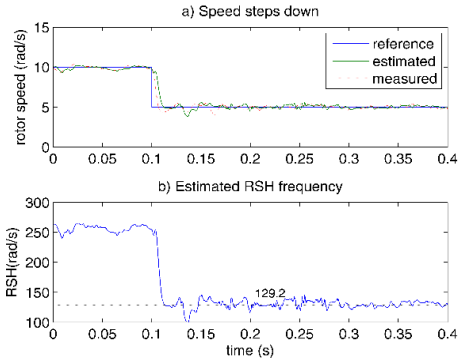


Fig. 9. Tracking capacity when speed step down at no-load

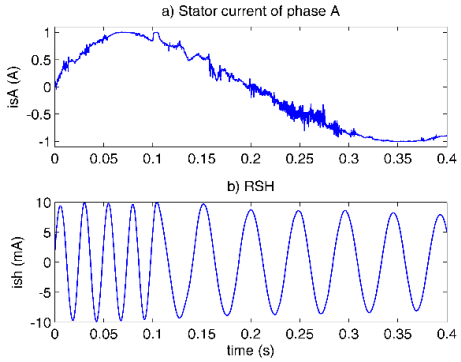


Fig. 10. Normalized phase current $i_{sA}$ and the output of filter $i_h$ when speed steps down at no-load

The steady-state performance of the MCA EXIN Pisarenko's method is shown in fig.11 and fig.12 , and the average speed estimation error is shown in Tab. 2.

In fig. 11, the machine operates at no-load, some reference speed are superimposed around the values 2, 4, 6, 8, 10 rad/s. The measured speeds and the estimated speeds are shown comparatively: the estimated speeds track the measured ones accurately, also in the very low speed range (see tab. 2), and even if the measured speed present some additional oscillations. In the 2 rad/s test, the estimated speed correctly tracks the measured ones. It should be remarked that this is a particularly challenging test, since 2 rad/s corresponds to about 1.3 % of the rated speed.

In fig. 12, the machine is 5Nm-loaded, and the reference speed varies from 10 rad/s to 2 rad/s. The results are similar to the no-load case. However, it has to be stressed that the steady-state tracking error is larger at 2 rad/s, since when the machine is loaded, other harmonics arise which are very close to the PSH, and can undesirably appear at the output of the ADALINEs. Better results is expected to be achieved by adopting a smaller sampling time, with consequent faster response.

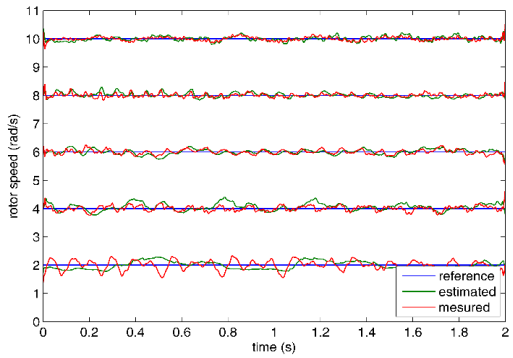


Fig. 11. speed tracking results at steady-state no load

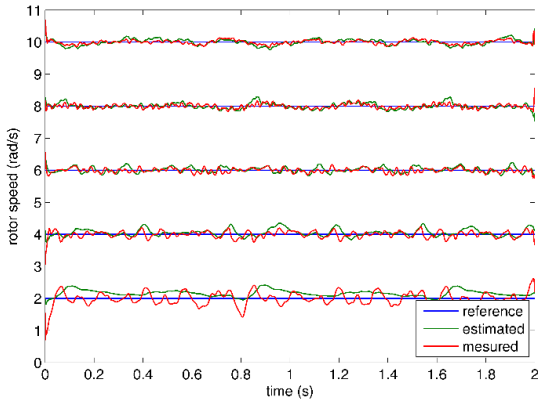


Fig. 12. speed tracking results at steady-state 5Nm load

TABLE II. AVERAGE SPEED ESTIMATION ERROR AT STEADY-STATE

| Ref speed (rad/s) | 2 | 4 | 6 | 8 | 10 |
|---|---|---|---|---|---|
| No load | 9.26% | 1.42% | 0.13% | 0.12% | 0.04% |
| 5Nm load | 7.96% | 1.35% | 0.26% | 0.06% | 0.02% |

## VII. CONCLUSIONS

This paper proposes a speed sensorless technique for induction motor drives based on the retrieval and tracking of the rotor slot harmonic**.** The speed related rotor slot harmonic is extracted from the stator phase current by two ADALINEs: one works in notch mode in order to eliminate the fundamental current, the other works in band mode thus its output consists only of the slot harmonic. The frequency of this extracted slot harmonic is then estimated by using the

MCA EXIN neural network based on Pisarenko's theory. The overall speed estimation algorithm is fast and accurate in a very wide speed range, and its performance has been verified both in the simulation and experiment on a suitably developed test set-up.

The proposed speed estimation algorithm has been integrated into a rotor flux oriented controlled induction motor drive, replacing the speed signal from the encoder. The proposed method has proven to be characterized by a very low sensitivity to the machine parameter variations, and no signal injection is required. Experimental results have proven that this sensorless technique permits the drive to work properly during speed step reference at very low speed and rated torque and, at speed steady-state, down to 1.3% of the rated speed.

## *REFERENCES*


[1] J. Holtz, "Sensorless control of induction machines—With or without signal injection?," IEEE Trans. Ind. Electron., vol. 53, no. 1, pp. 7–30, Feb. 2006.

[2] P. Vas, "Sensorless Vector and Direct Torque Control", Oxford Science Publication, 1998.

[3] Barut M, Bogosyan S, Gokasan M. Speed-sensorless estimation for induction motors using extended Kalman filters[J]. Industrial Electronics, IEEE Transactions on, 2007, 54(1): 272-280.

[4] Harnefors L, Hinkkanen M. Complete stability of reduced-order and full-order observers for sensorless IM drives[J]. Industrial Electronics, IEEE Transactions on, 2008, 55(3): 1319-1329.

[5] Guzinski, J.; Abu-Rub, H., "Speed Sensorless Induction Motor Drive With Predictive Current Controller," Industrial Electronics, IEEE Transactions on , vol.60, no.2, pp.699,709, Feb. 2013

[6] Xi Zhang, "Sensorless Induction Motor Drive Using Indirect Vector Controller and Sliding-Mode Observer for Electric Vehicles," Vehicular Technology, IEEE Transactions on , vol.62, no.7, pp.3010,3018, Sept. 2013

[7] Zengcai Qu; Hinkkanen, M.; Harnefors, L., "Gain Scheduling of a Full-Order Observer for Sensorless Induction Motor Drives," Industry Applications, IEEE Transactions on , vol.50, no.6, pp.3834,3845, Nov.-Dec. 2014

[8] Vogelsberger, M.A.; Grubic, S.; Habetler, T.G.; Wolbank, T.M., "Using PWM-Induced Transient Excitation and Advanced Signal Processing for Zero-Speed Sensorless Control of AC Machines," Industrial Electronics, IEEE Transactions on , vol.57, no.1, pp.365,374, Jan. 2010

[9] Young-Su Kwon; Jeong-Hum Lee; Sang-Ho Moon; Byung-Ki Kwon; Chang-Ho Choi; Jul-Ki Seok, "Standstill Parameter Identification of Vector-Controlled Induction Motors Using the Frequency Characteristics of Rotor Bars," Industry Applications, IEEE Transactions on , vol.45, no.5, pp.1610,1618, Sept.-oct. 2009

[10] Foo G, Rahman M F. Sensorless sliding-mode MTPA control of an IPM synchronous motor drive using a sliding-mode observer and HF signal injection[J]. Industrial Electronics, IEEE Transactions on, 2010, 57(4): 1270-1278.

[11] Zhu Z Q, Gong L M. Investigation of effectiveness of sensorless operation in carrier-signal-injection-based sensorless-control methods[J]. Industrial Electronics, IEEE Transactions on, 2011, 58(8): 3431-3439.

[12] Accetta, A.; Cirrincione, M.; Pucci, M.; Vitale, G., "Sensorless Control of PMSM Fractional Horsepower Drives by Signal Injection and Neural Adaptive-Band Filtering," Industrial Electronics, IEEE Transactions on , vol.59, no.3, pp.1355,1366, March 2012

[13] P. L. Jansen, R. D. Lorenz, "Transducerless Field Orientation Concepts Employing Saturation-Induced Saliencies in Induction Machines", IEEE Transactions on Industry Applications, vol. 32, n. 6, 1380-1393, November/December 1996.

[14] A. Consoli, G. Scarcella, A. Testa, " Speed- and current-sensorless field-oriented induction motor drive operating at low stator frequencies ", IEEE Trans. on Ind. Appl., vol. 40, n. 1 , pp:186 – 193, Jan.-Feb. 2004.

[15] Blasco-Gimenez, R.; Asher, G.M.; Sumner, M.; Bradley, K.J., "Performance of FFT-rotor slot harmonic speed detector for sensorless induction motor drives," Electric Power Applications, IEE Proceedings - , vol.143, no.3, pp.258,268, May 1996

[16] Hurst, K.D.; Habetler, T.G., "A comparison of spectrum estimation techniques for sensorless speed detection in induction machines," Industry Applications Conference, 1995. Thirtieth IAS Annual Meeting, IAS '95., Conference Record of the 1995 IEEE , vol.1, no., pp.553,559 vol.1, 8-12 Oct 1995

[17] Nishibata, K.; Ishida, M.; Doki, S.; Masuzawa, T.; Fujitsuna, M., "Speed Estimation Method utilizing Rotor Slot Harmonics Detected from Line Current for Speed Sensorless Drive of Ultra High Speed Induction Machine," Industrial Technology, 2006. ICIT 2006. IEEE International Conference on , vol., no., pp.1591,1596, 15-17 Dec. 2006

[18] Aiello, M.; Cataliotti, A.; Nuccio, S., "An induction motor speed measurement method based on current harmonic analysis with the chirp-Z transform," Instrumentation and Measurement, IEEE Transactions on , vol.54, no.5, pp.1811,1819, Oct. 2005

[19] Ferrah, A.; Bradley, K.J.; Hogben-Laing, P.J.; Woolfson, Malcolm S.; Asher, G.M.; Sumner, M.; Cilia, J.; Shuli, J., "A speed identifier for induction motor drives using real-time adaptive digital filtering," Industry Applications, IEEE Transactions on , vol.34, no.1, pp.156,162, Jan/Feb 1998

[20] Zhi Gao; Turner, L.; Colby, R.S.; Leprettre, B., "A Frequency Demodulation Approach to Induction Motor Speed Detection," Industry Applications, IEEE Transactions on , vol.47, no.4, pp.1632,1642, July-Aug. 2011

[21] Keysan, O.; Ertan, H.B., "Real-Time Speed and Position Estimation Using Rotor Slot Harmonics," Industrial Informatics, IEEE Transactions on , vol.9, no.2, pp.899,908, May 2013

[22] M. Cirrincione , M. Pucci , G. Cirrincione , A. Miraoui, "Space-Vector State Model of Induction Machines Including Rotor Slotting Effects: Towards a New Category of Observers", IEEE Transactions on Industry Applications, Vol. 44, n.6, November/December 2008.

[23] Cirrincione M, Pucci M, Vitale G. A single-phase DG generation unit with shunt active power filter capability by adaptive neural filtering[J]. Industrial Electronics, IEEE Transactions on, 2008, 55(5): 2093-2110.

[24] M. Cirrincione, M. Pucci, G. Vitale, A. Miraoui, "Current Harmonic Compensation by a Single-Phase Shunt Active Power Filter Controlled by Adaptive Neural Filtering", IEEE Transactions on Industrial Electronics, Vol. 56, n. 8, August 2009

[25] B. Widrow, S. D. Stearns, Adaptive Signal Processing, Signal Processing Series, Prentice-Hall, Englewood Cliffs, NJ, 1985.

[26] Cirrincione, G.; Cirrincione, M.; Herault, J.; Van Huffel, S., "The MCA EXIN neuron for the minor component analysis," Neural Networks, IEEE Transactions on , vol.13, no.1, pp.160,187, Jan 2002

[27] S. Van Huffel and J. Vandewalle, Analysis of the Total Least Squares Problem and Its Use in Parameter Estimation. Leuven, Belgium: SIAM, 1987.

[28] Rodríguez, P.; Luna, A.; Muñoz-Aguilar, R.S.; Etxeberria-Otadui, I.; Teodorescu, R.; Blaabjerg, F., "A Stationary Reference Frame Grid Synchronization System for Three-Phase Grid-Connected Power Converters Under Adverse Grid Conditions," Power Electronics, IEEE Transactions on , vol.27, no.1, pp.99,112, Jan. 2012

[29] Golestan, S.; Monfared, M.; Freijedo, F.D.; Guerrero, J.M., "Dynamics Assessment of Advanced Single-Phase PLL Structures," Industrial Electronics, IEEE Transactions on , vol.60, no.6, pp.2167,2177, June 2013

[30] Hayes M H. Statistical digital signal processing and modelling [M]. John Wiley & Sons, 2009.

[31] Kay, Steven M., and Stanley Lawrence Marple Jr. "Spectrum analysis—a modern perspective." Proceedings of the IEEE 69.11 (1981): 1380-1419.

[32] Stoica, Petre, Jian Li, and Xing Tan. "On spatial power spectrum and signal estimation using the Pisarenko framework." Signal Processing, IEEE Transactions on 56.10 (2008): 5109-5119.